Title
Energy-saving opportunities of direct-DC loads in buildings

Authors
Gerber, Daniel L
Liou, Richard
Brown, Richard

Publication Date
2019-08-01

DOI
10.1016/j.apenergy.2019.04.089

Peer reviewed

Energy-Saving Opportunities of Direct-DC Loads in Buildings

Daniel L. Gerber[a,*], Richard Liou[a], Richard Brown[a]

[a]*Lawrence Berkeley National Laboratory, Building 90, 1 Cyclotron Rd, Berkeley, CA 94720*

Abstract

Despite the recent interest in direct current (DC) power distribution in buildings, the market for DC-ready loads remains small. The existing DC loads in various products or research test beds are not always designed to efficiently leverage the benefits of DC. This work addresses a pressing need for a study into the development of efficient DC loads. In particular, it focuses on documenting and demonstrating how to best leverage a DC input to eliminate or improve conversion stages in a load's power converter. This work identifies how typical building loads can benefit from DC input, including bath fans, refrigerators, wall adapters, task lights, and zone lighting. It then details the development of several prototypes that demonstrate efficiency savings with DC. The most efficient direct-DC loads are explicitly designed for DC from the ground up, rather than from an AC modification.

Keywords: DC distribution, plug loads, direct DC, buildings, variable frequency drive, LED lighting

1. Background and Motivation

1.1. Motivation for DC Distribution in Buildings

Direct current (DC) power distribution systems have become a recent topic in building energy research as a means of reducing power consumption. In the past, alternating current (AC) was well suited to power the nineteenth and twentieth century loads such as incandescent lamps, resistive heating, and fixed speed motors. However, with the proliferation of electronics, light emitting diode (LED) lighting, and variable frequency drives (VFDs) for motor-driven loads, an increasing fraction of todays electric loads operate internally on DC [1]. In addition, the recent growth in

*Corresponding author

Email addresses: dgerb@berkeley.edu (Daniel L. Gerber), rliou92@lbl.gov (Richard Liou), rebrown@lbl.gov (Richard Brown)

on-site photovoltaic (PV) generation [2] and battery storage [3] adds even more DC electronics to the building network. DC power distribution for on-site generation, storage, and loads can reduce losses in converting between AC and DC, leading to electricity savings across the board [4].

The potential electricity savings from DC distribution systems in buildings have been addressed in numerous studies [5–27]. For the commercial building sector, the reported savings vary widely from 2% [6] to as much as 19% [7]. Gerber et al. [21] performed a series of highly-detailed parametric simulations that varied solar and storage capacity in several equivalent AC and DC buildings. The results suggested that the highest savings occur in buildings with large PV and storage capacities, such as zero net energy buildings. An additional loss analysis revealed that low-power load rectifiers contributed the most loss in the AC buildings. In general, the reported savings are highly dependent on the system topology, converter efficiencies, distribution voltage levels, and the coincidence of generation and load.

Systems with 380 V DC distribution have been proposed and successfully implemented in data centers. Fig. 1 shows a typical high-level DC architecture. The estimated savings between 7% and 28% are a result of the load being predominantly electronics [5]. Commercial buildings have seen several instances of early adoption for DC distribution systems, primarily in lighting applications [27–29]. Several other experiments developed DC loads and test beds to evaluate the savings and power quality with DC [25–27, 30, 31]. Weiss et al. [25] used measured efficiency data in a variety of loads to estimate the DC savings at 5%. Fregosi et al. [27] performed a similar analysis on lighting test beds with the Bosch DC microgrid, resulting in savings of 6% to 8%. Finally, Boeke and Wendt [26] reported 2% measured and 5% potential electricity savings from an office LED lighting test bed at the Philips High Tech Campus in Eindhoven, Netherlands. Many of these experimental DC loads and test beds exhibit significantly lower savings than those predicted by past analyses and simulations. This work suggests ways in which experimental loads in DC test beds can be improved.

1.2. Previous Works in DC Modification

Currently, there is a small market for DC plug loads for RV and boating applications [32]. These loads are often compact and designed for 12 V or 24 V DC from the vehicle's battery. In the next few decades, this market will expand to low-voltage DC solar home systems in developing countries that currently lack universal electrification.

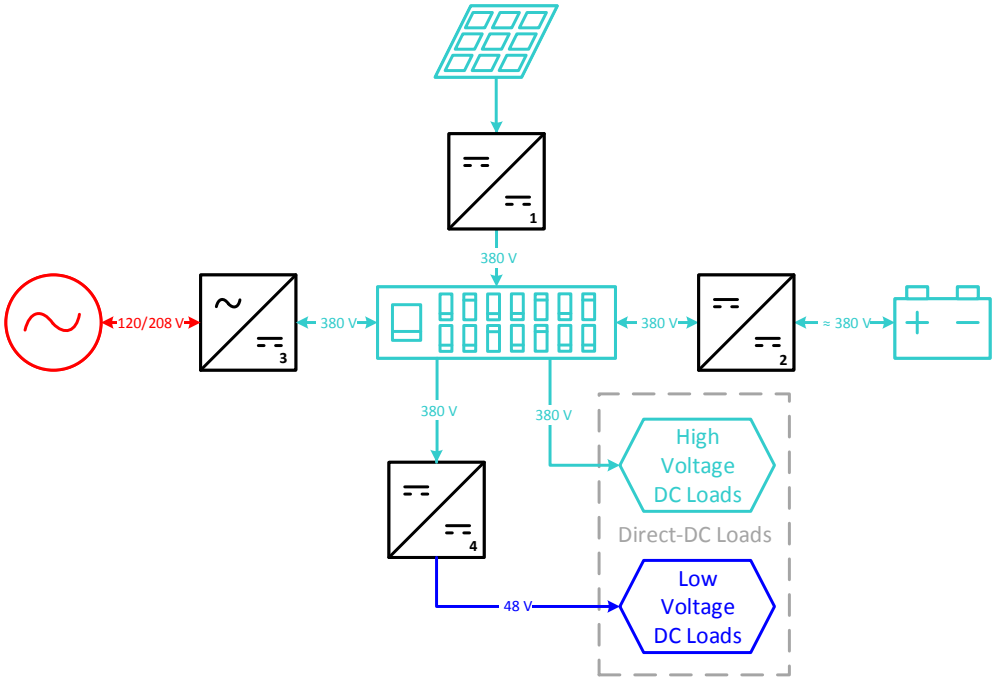

Figure 1: Example DC building topology with distribution at 48 and 380 V DC. Converters: 1. MPPT power optimizer, 2. integrated battery charge controller, 3. grid tie inverter, 4. PoE switch. Certain loads such as LEDs may require an additional DC-DC converter at the load (not shown).

Several previous works have prototyped DC plug loads for newly constructed DC buildings in the residential and commercial sectors. Many of these efforts create prototypes for a variety of DC appliances as a means of performing system or microgrid tests [33–37]. Recent research has produced DC prototypes in many end-use categories such as lighting [25, 26, 34–38], motor loads [34, 36, 37, 39–42], electronics [34–37, 43], and induction cooking [35, 44].

Despite the wealth of research on developing DC loads, there are still several important gaps. First, many of the previous works compare AC and DC loads of different technologies. It has been common, for example, to compare a DC variable frequency drive motor appliance to an outdated AC synchronous fixed-speed motor. Second, many of the previous prototypes are not designed to operate at the DC distribution voltages and require DC/DC converters at the input. Such practice neglects the many design optimizations allowed by DC that can benefit efficiency and cost. Finally, most of the previous studies use prototype DC plug loads, but do so as a means of showcasing another research topic such as a DC microgrid demonstration or a new control strategy.

This work aims to improve on previous works by focusing on the optimal development of DC loads. It introduces several new concepts and analyses, including:

- A formal categorization of building end-use loads by how they benefit from DC distribution
- An analysis that shows how standard variable speed motors can be improved and optimally designed for DC input
- Two completely new system topologies for efficiently powering LEDs from DC distribution

The main purpose of this work is to suggest ideas and practices that can and should be implemented in future products. It gives detailed explanations of the benefits of DC from the load perspective.

2. DC Load Modifications

2.1. Existing DC Voltage Standards

There are several considerations in selecting the DC distribution voltage. First and foremost is electrical safety, and OSHA standard 1910.303(g)(2)(i) [45] considers voltages below 50 V AC or DC to be touch-safe (the UK IET BS 7671:2008 [46] specifies it at 50 V AC and 120 V DC). Second, higher voltages require more insulation to protect against dielectric breakdown. Finally, low-voltage systems can experience high wire loss and voltage drop. For a device with constant power requirements P_L, the current can be expressed as $I = P_L/V$. Since the wire loss $P_w = I^2 R_w$ decreases quadratically with the wire's voltage, high-power devices are often wired on high-voltage lines.

This work investigates several existing or emerging standards for DC plug voltages:

- USB Type C: 5-20 V, 100 W
- PoE: 48-56 V, 100 W
- EMerge Alliance Data/Telecom Center Standard: 380 V

These standards are further described in Appendix A.

2.2. Devices that Benefit from DC

Internally DC loads are classified as being direct-DC or native-DC, depending on whether the building distribution is DC or AC, respectively [6]. Direct-DC loads connect to the DC network directly or through a DC/DC converter. Native-DC loads always require a rectifier to interface with the AC distribution.

This work further classifies loads based on how they can benefit from an interface to a DC distribution network. In Fig. 2, common plug loads are classified as being:

- DC-connected: The internal DC stage of these loads can be connected or hardwired directly to the DC network. A direct-DC input would bypass the input voltage conversion (and/or rectification) stage, thus allowing for savings in efficiency and cost. DC benefits these loads the most.

- DC-converted: The internal DC stage of these loads requires a DC/DC converter in order to connect to the DC network. However for most loads, the direct-DC version outperforms its

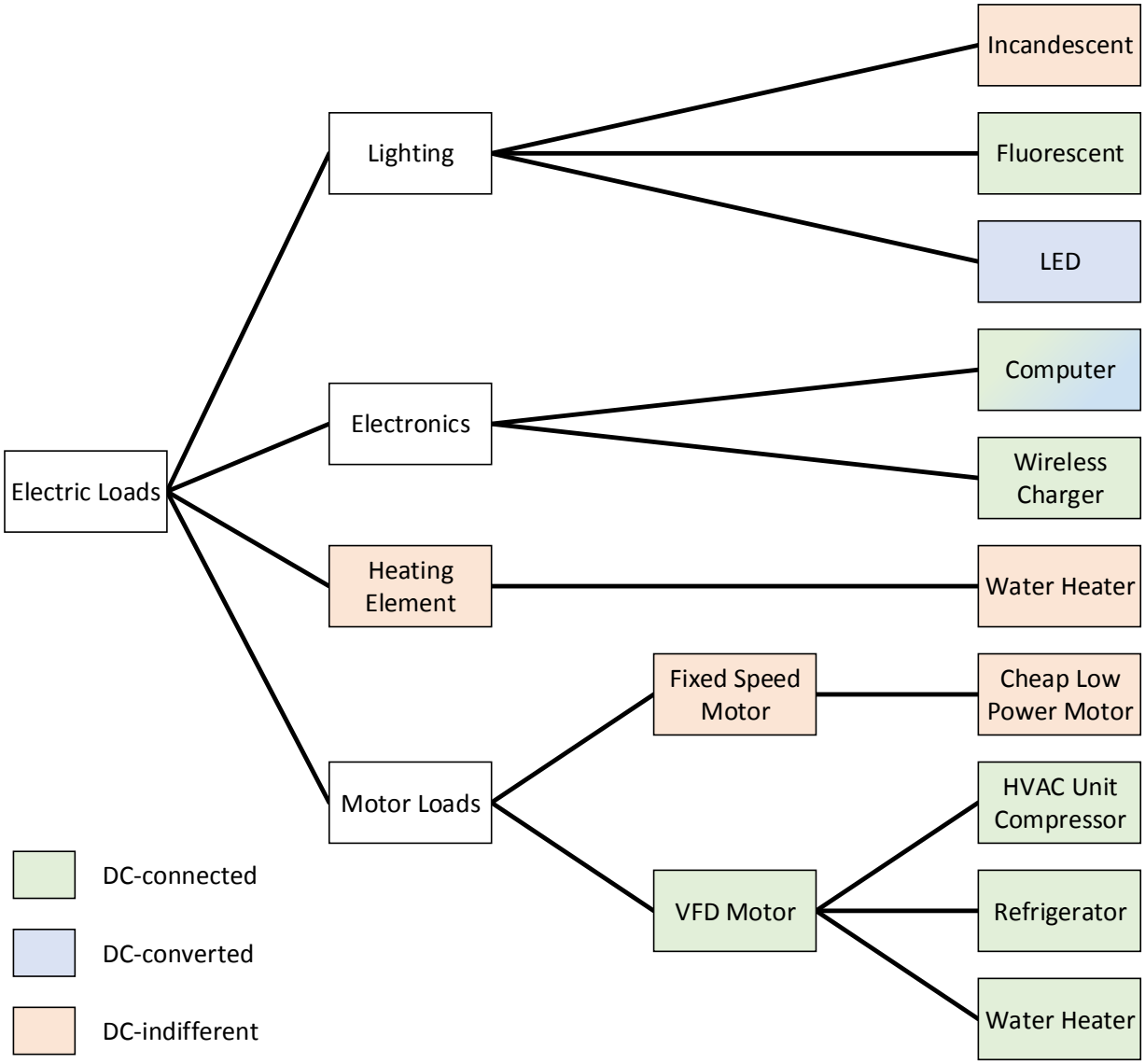

Figure 2: DC-connected loads have an internal DC stage that can be connected or hardwired to DC distribution. DC-converted loads require an input DC/DC converter, but still benefit from a DC input. DC-indifferent loads do not benefit from a DC input.

native-DC counterpart in efficiency, cost, and size. DC offers some benefits for these loads.

- DC-indifferent: The load can be hardwired to an AC or DC distribution with equivalent cost and efficiency. DC does not directly benefit these loads.

2.2.1. DC-connected

Includes loads with a fixed internal DC bus, many of which require AC power at a non-mains frequency.

VFD motor loads contain a brushless DC (BLDC) inverter-driven synchronous or asynchronous motor. Due to their efficiency benefits, VFDs will eventually replace fixed-speed motors in air conditioners, refrigerators, heat-pump air and water heaters, and ventilation fans [47–49]. As shown in Fig. 3a, native-DC VFD motors require a rectification stage, followed by a DC capacitor bus. The inverter supplies the stator coils with a variable-frequency AC drive. In well-designed direct-DC VFDs, the DC capacitor bus could be connected directly to the DC distribution, as shown in Fig. 3b. A direct connection bypasses the rectification stage, thus allowing for savings in efficiency and cost. In addition, the DC bus capacitors can be reduced, as described in Appendix

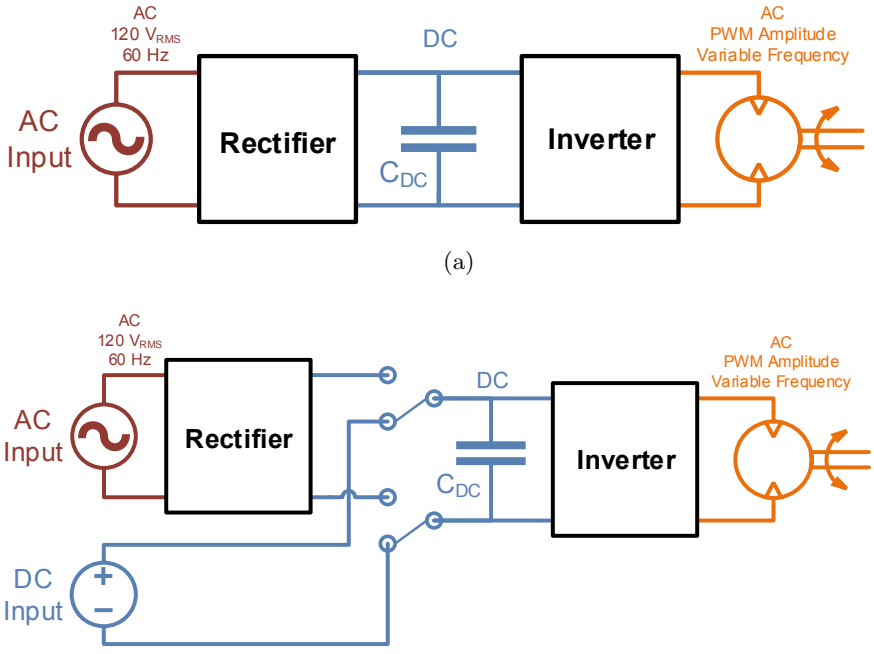

Figure 3: Block schematic of a VFD motor, as present in the refrigerator and bathroom fan. The inverter is powered from an internal DC stage (blue), and outputs AC at a variable frequency (orange). (a) A rectifier is required to convert 60 Hz AC (red) to DC. (b) A proposed modification, with multiplexed AC and DC inputs.

C. Although they are still required for electromagnetic compatibility, they do not need to filter AC mains frequency power ripple.

Wireless transmitters power an antenna with high-frequency AC. In this way, wireless transmitters are structurally similar to VFDs: they contain a rectifier, a DC stage, and a power amplifier, which outputs AC at the antenna's resonant frequency. Transmitters are present in any wirelessly connected plug-loads, including routers, computers, and Internet of Things devices. Other applications, such as wireless chargers and induction stoves employ near-field wireless power transfer.

2.2.2. DC-converted

Includes current-controlled loads and loads with multiple internal voltage rails.

LEDs are a current-controlled load since their luminosity is nearly proportional to their current. DC LED drivers are often 95-98% efficient, whereas AC LED drivers commonly have 86-93% efficiency [21, 27]. In addition, AC LED drivers are more expensive because they have to rectify the AC input, apply power factor correction (PFC), and cancel the 120 Hz AC power ripple with a large electrolytic capacitor.

Laptops require several DC/DC converters to power the internal components at their respective voltages. Nonetheless, an AC/DC wall adapter is also required to supply the laptop's primary power rail. DC input to the primary rail could obviate the need for a wall adapter, allowing for benefits similar to DC-connected devices.

2.2.3. DC-indifferent

Includes heating elements and fixed-speed motors. Resistive heating elements are often found in water heaters, ovens, and incandescent bulbs. These devices can be connected to AC or DC distributions with equal efficiency. Fixed-speed motors are often found in old or inexpensive motor loads. Due to their low efficiency in many applications, they will eventually be replaced by VFDs.

2.3. Experimental Method

This work examines a bathroom fan, refrigerator, wall adapter, LED task lamp, and LED zone lighting rig. These loads are selected to represent the end-use categories of ventilation, refrigeration, electronics, and lighting in residential or small commercial buildings. The prototypes and modifications are intended to demonstrate savings by leveraging a DC input to reduce the number of conversion stages. The method of reporting savings varies by load, and includes measuring the

input power consumption, nominal operating efficiency, and efficiency curves. Efficiency measurements use $\eta = P_{out}/P_{in}$, where P_{out} is the power measured at the device's internal DC stage, and P_{in} is measured at the AC or DC input.

3. Bath Fan

3.1. Modifications for DC Input

As described in Sec. 2.2, variable frequency drive (VFD) loads have an internal DC capacitor that buffers the inverter. There are two proposed modifications to the Delta GBR80 bath fan. The 48 V DC-converted modification in Fig. 4b is intended for PoE, and the 12 V DC-connected modification in Fig. 4c is for USB-C. Although PoE requires a 48/12 V DC/DC conversion, it is practical due to the distance limitations of USB-C. These modifications both maintain the DC bus at its nominal 12 V, since increasing or decreasing the bus voltage may damage the inverter or stator coils, respectively. As such, this experiment does not affect the motor's speed and torque.

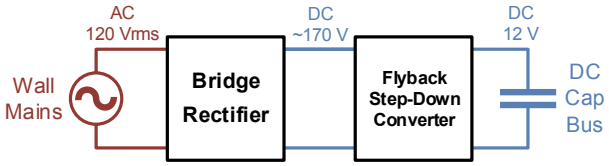

(a)

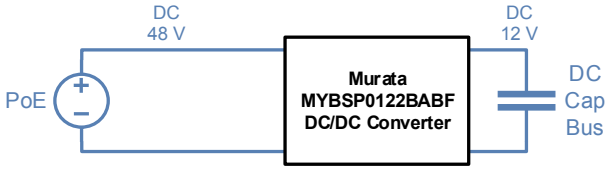

(b)

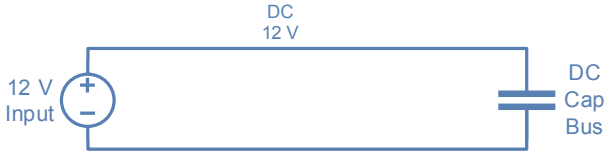

(c)

Figure 4: Methods of providing power to the bath fan's DC capacitor bus and inverter stages. (a) The fan's original AC/DC rectifier board, shown in Fig. 6a. (b) The DC-converted modification for 48 V PoE input, using a DC/DC converter, shown in Fig. 6b. (c) A DC-connected modification for a hypothetical 12 V DC input. This configuration represents how DC input would be beneficial if the motor and inverter were designed for 48 V DC.

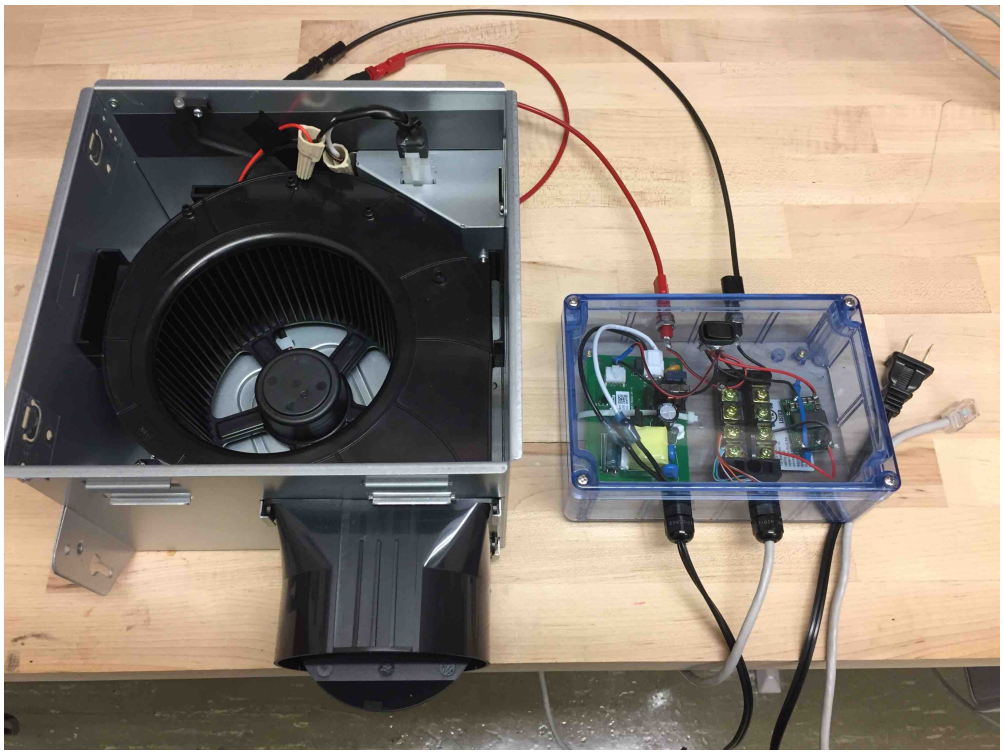

Figure 5: Prototype of the Delta GBR80 bath fan, modified to accept a PoE input. The blue box contains the boards in Fig. 6, with a switch to toggle between AC or DC input.

3.2. Experimental Prototype and Results

As shown in Fig. 5, the bath fan prototype has a multiplexed AC or DC input. The original rectifier board in Fig. 6a uses an isolated flyback topology. The DC-converted input uses the Murata MYBSP0122BABF isolated 48/12 V DC/DC converter in Fig. 6b.

The results suggest that direct-DC can improve the fan's power consumption. The efficiency curves in Fig. 7 show that the DC/DC converter is up to 6% more efficient than the original rectifier board. Tab. 1 shows a decrease in the fan's input power with DC input. In addition, the fan draws even less power with a 12 V input, which represents the savings potential of a DC-connected design. In this experiment, the exhaust valve is held open or shut to simulate a lightly or heavily loaded fan, respectively.

3.3. Discussion

The 48 V DC-converted modification improves upon the efficiency of the rectifier board. Not only does it remove the AC/DC rectification stage, but it also allows for a smaller DC/DC conversion ratio V_{out}/V_{in}. Large conversion ratios require the switching elements to frequently block power flow to the load, yet the converter still suffers parasitic loss regardless. The 120 V_{RMS} AC

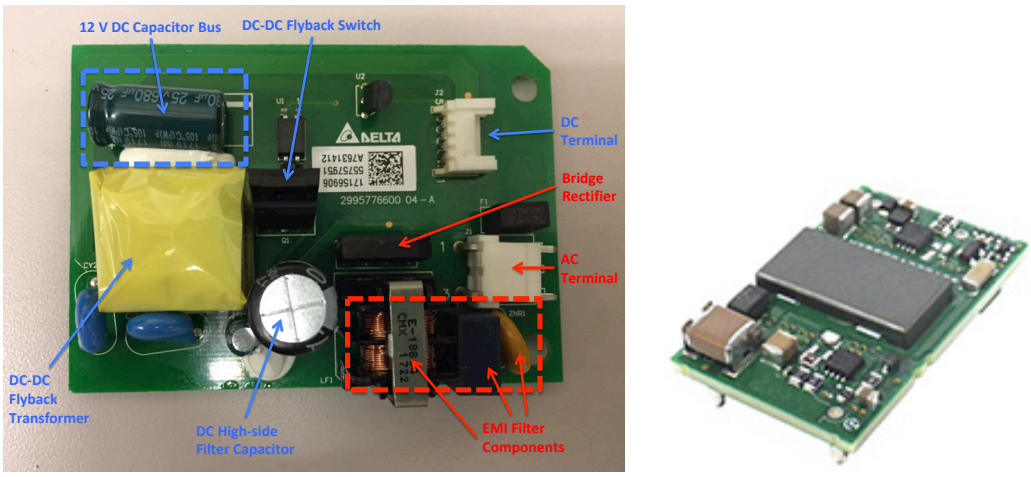

(a) (b)

Figure 6: Input power conversion boards for the Delta bath fan. (a) The original rectifier board that converts 120 V_{RMS} AC to 12 V DC. The board dimensions are 8 x 6 cm. (b) A Murata MYBSP0122BABF 48/12 V DC/DC converter for interfacing the DC capacitor stage with PoE. The board dimensions are 3.5 x 2 cm.

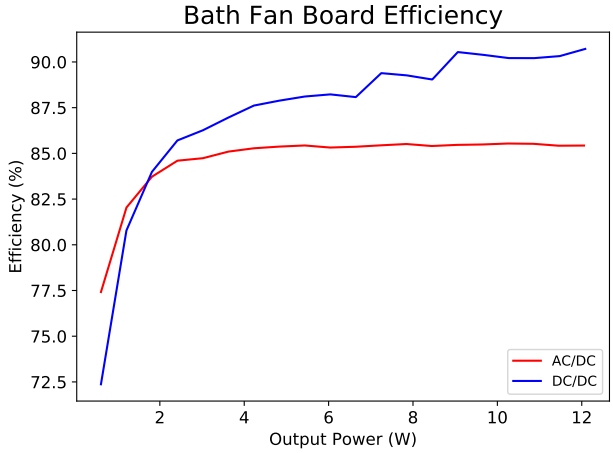

Figure 7: Efficiency curves for the prototype bath fan's AC/DC and DC/DC boards.

converter board mitigates some of this loss by instead converting through the flyback transformer's turns ratio. However, inclusion of a flyback transformer adds cost, size, core loss, and winding loss.

Although the 12 V DC-connected modification has the lowest cost and consumption, it is impractical for a bath fan due to low-voltage wire loss. Nonetheless, the 12 V modification is explicitly intended to show the benefits of a DC-connected design. Ideally, a PoE bath fan would use a 48 V inverter and motor. Appendix B shows how a BLDC motor can be redesigned to operate with a different internal DC voltage.

Table 1: Fan prototype power consumption

Input Type	Conversion	Input Power Light Load	Input Power Heavy Load	AC Power Factor
Original 120 V_{RMS} AC	AC/DC	7.75 W	9.01 W	0.64
DC-converted 48 V DC	DC/DC	7.43 W	8.65 W	N/A
DC-connected 12 V DC	None	6.6 W	7.72 W	N/A

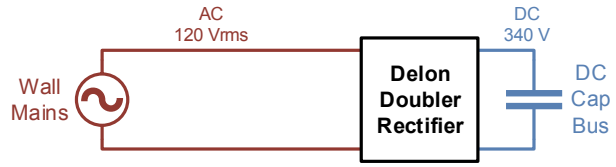

(a)

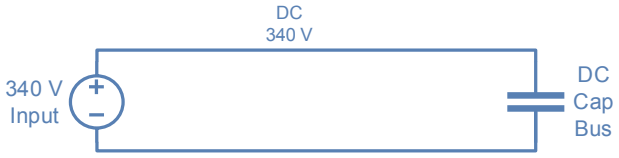

(b)

Figure 8: Methods of providing power to the refrigerator's DC capacitor bus and inverter stages. (a) The refrigerator's original AC/DC Delon doubler rectifier circuit. (b) The DC-connected modification for 340 V input, which approximately represents 380 V DC.

4. Refrigerator

4.1. Modifications for DC Input

Like the bath fan, the DC input modification of the 11 ft^3 LG LTNC11121V inverter-based refrigerator removes the VFD rectification stage. The main difference is that the refrigerator's rectifier is a Delon (full wave) doubler, whose unloaded DC output is 340 V DC. As such, the refrigerator is modified to accept a 340 V DC input, which although not a standard DC voltage, approximates the efficiency and power draw at 380 V DC.

4.2. Experimental Prototype and Results

The refrigerator prototype, shown in Fig. 9, adds a 340 V DC-connected input to the DC capacitor stage. As shown in Fig. 10 the inverter board's original AC input contains an input EMI filter and protection components. The DC prototype instead contains a thermistor that protects

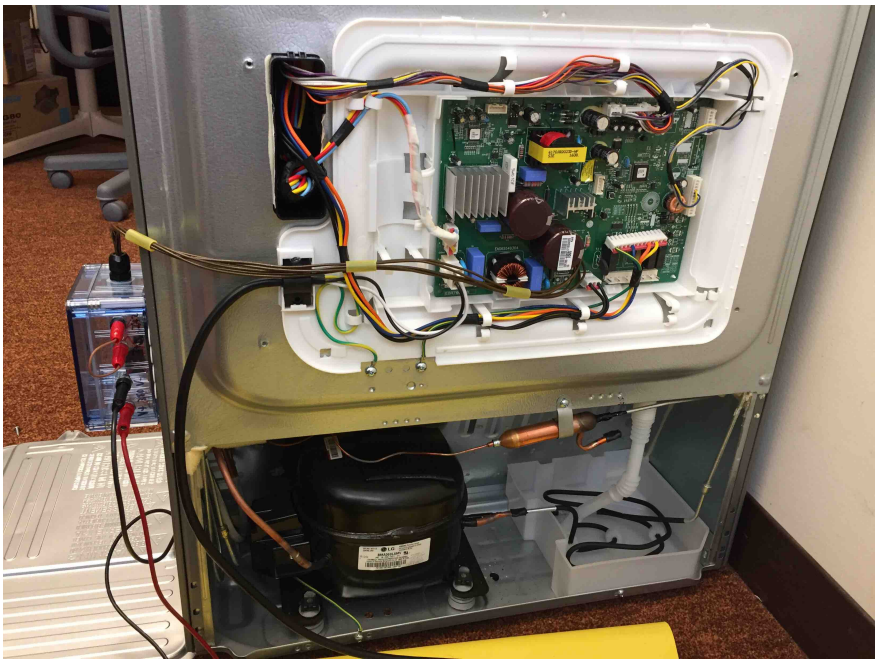

Figure 9: Prototype for the DC input modification of a refrigerator. The blue box on the left side allows for a 340 V DC input to the inverter board's DC capacitor bus. The compressor is the BMA069LAMV model.

the DC capacitors from over-current at start-up. In this experiment, the refrigerator's defrost coils have been deactivated, and power is drawn solely by the compressor and electronics.

The efficiency of the rectification stage in Fig. 8a is 99%, averaged over fifty measurements with power ranging from 50 W to 80 W. There is little to no correlation between power and efficiency in this range. The AC power factor is 0.65, and is caused entirely by harmonic distortion.

4.3. Discussion

The refrigerator barely benefits from a high-voltage DC input, since bypassing the rectification stage only saves 1% of the input power. 340 V operation can be very efficient, but requires the large inverter and capacitors shown in Fig. 10. In contrast, many low-voltage DC refrigerators can operate with smaller electronics, such as the 24 V Danfoss 101N0212 in Fig. 11. Compared to the LTNC11121V, its compressor has fewer and thicker windings, as discussed in Appendix B.

It is important to note that the LNTC11121V has a poor power factor of 0.65 due to its lack of power factor correction (PFC). Although inverter-based refrigerators are generally subject to the stringent IEC 61000-3-2 Class D harmonic specifications, these requirements only apply for devices that draw more than 75 W of power [50, 51]. While the LG refrigerator sometimes draws up to 80 W, it usually operates below 75 W (the defrost coils draw up to 175 W, but they are a resistive

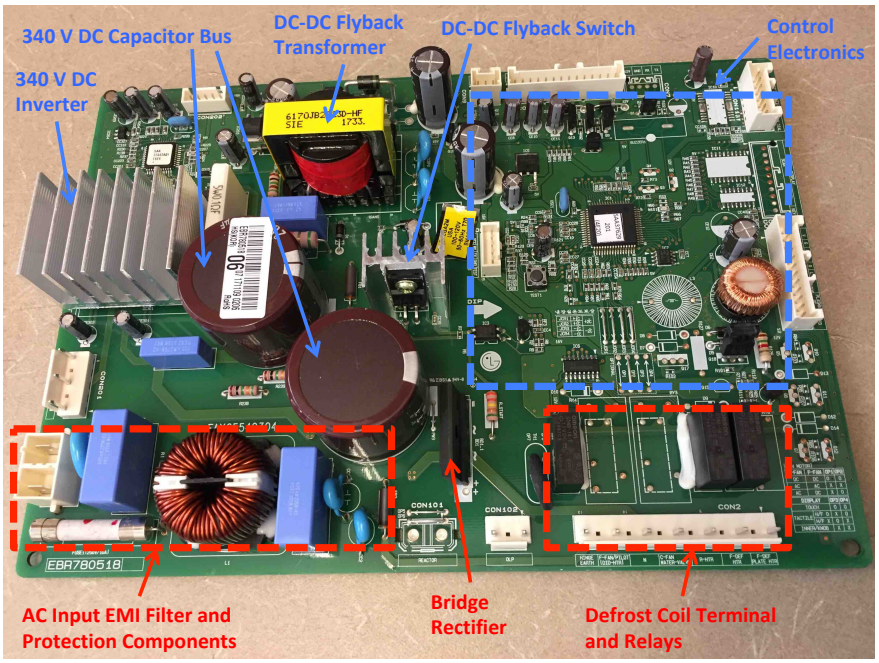

Figure 10: Inverter board for the LG LTNC11121V refrigerator. The inverter is a high-voltage 3-phase SIM6822M chip. The board dimensions are 23 x 16 cm.

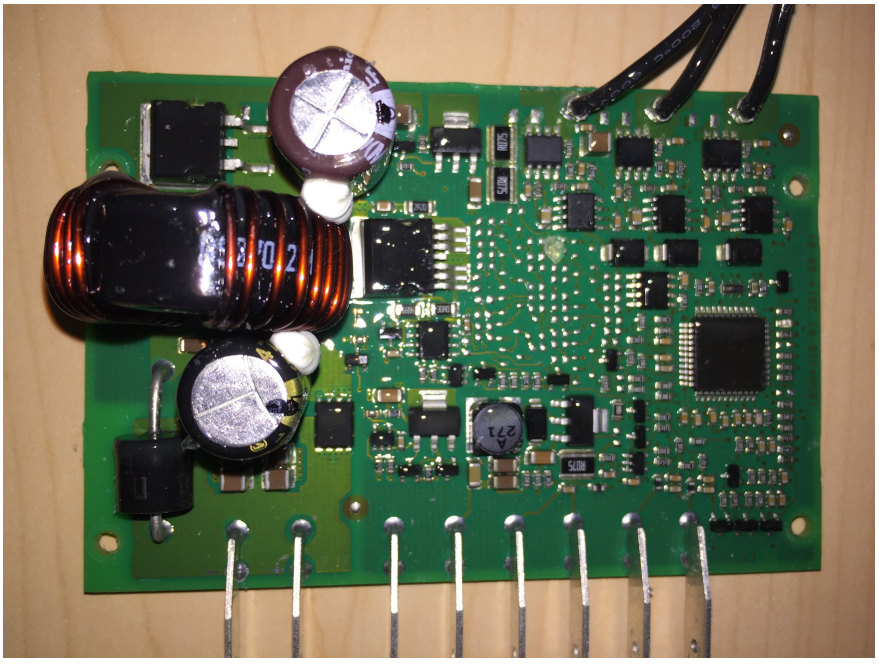

Figure 11: Danfoss/Secop 101N0212 inverter board, for a Danfoss 12/24 V DC refrigerator. The board dimensions are 10 x 6.5 cm. This inverter board can provide up to 113 W when connected to a BD50F compressor at 3500 RPM and 30°C ambient temperature.

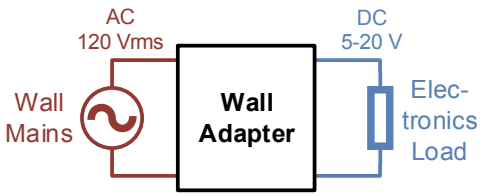

(a)

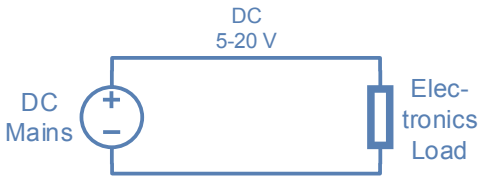

(b)

Figure 12: Two different methods for powering the internal DC bus in electronics. (a) Native-DC electronics require a wall adapter, which often rectifies 120 V AC to 170 V DC and steps-down to the 5-20 V DC appropriate for electronics. (b) This work considers direct-DC electronics to be DC-connected.

load with unity power factor). Standard-sized refrigerators would require a PFC rectifier, whose losses and cost are much greater than the Delon rectifier. For these refrigerators, a DC-connected input would be considerably more beneficial.

DC input allows for a reduction in the size of the DC capacitor bus. Not only are the high-voltage high-capacitance electrolytics in Fig. 10 bulky and expensive, but they are also prone to failure and may limit the life span of the entire board [52, 53]. The DC capacitors are sized to filter 120 Hz AC power ripple, provide an energy buffer for rapid changes in motor torque, and filter the high-frequency inverter PWM ripple. Appendix C describes how the giant DC capacitors in Fig. 10 are mainly required for filtering the 120 Hz AC power ripple, and can be greatly reduced with direct-DC.

5. Wall Adapters

5.1. Modifications for DC Input

Wall adapters provide low-voltage DC to many household plug-load electronics. Future trends in electronics and the Internet of Things will see an increase in distributed AC/DC wall adapters. In general, low-power units with high voltage-conversion ratios are often inefficient. The US only requires wall adapters to be 74% to 88% efficient, depending on power level [54, 55]. DC distribution is attractive because it can eliminate the wall adapter, improving efficiency, overall cost, and convenience.

This work studies the losses in native-DC electronics by measuring the efficiency of several USB-C wall adapters. As shown in Fig. 12, this work considers direct-DC electronics as being DC-connected. In this sense, the savings with DC is equal to the wall adapter's measured loss. Other more realistic scenarios may require a DC wall adapter, which is further discussed in Section 5.3.

5.2. Experimental Prototype and Results

The five USB-C wall adapters, shown in Table 2, vary in power capacity and quality. These adapters are loaded with a 5 V Anker Powerpack battery and a Macbook that attempts to request up to 20 V. The efficiency is calculated from ten-minute measurements of the input and output energy.

Table 2: Wall adapter efficiency

Adapter	Output Voltage (V)	Efficiency (%)	Average Measurement Output Power (W)
Choetech 15 W	5	84.73	15.7
Pixel 18 W	5	87.18	11.0
	9	88.24	17.6
Anker 30 W	5	90.82	10.7
	20	91.22	29.2
Choetech 39 W	5	87.15	10.4
	15	91.96	37.7
Macbook 87 W	5	89.92	10.6
	20	94.91	59.8

5.3. Discussion

The results in this study show that wall adapters contribute significantly to the AC system loss. However, direct-DC electronics would more realistically be DC-converted, since building distribution voltage must be greater than 5-20 V to avoid wire loss. As such, direct-DC electronics will require a DC/DC wall adapter with a potentially large step-down ratio. Nonetheless, DC distribution allows for highly-efficient centralized conversions. For example, a single centralized direct-DC charging station could power all the electronics in a quad of cubicles. High-power converters such as the 800 W Vicor BCM6123xD1E1368yzz perform a 380/12 V DC conversion with 97% efficiency.

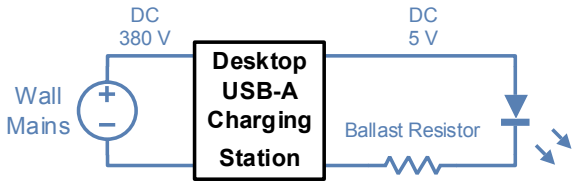

(a)

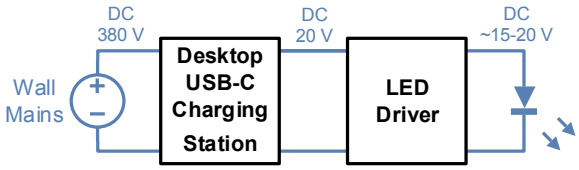

(b)

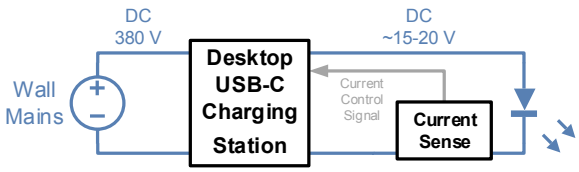

(c)

Figure 13: Methods of powering a task lamp with DC input from a desktop charging station. Note that the wall mains could also be 120 V_{RMS} AC or 48 V DC. (a) Use a ballast resistor for current control. (b) Connect the LED driver in the lamp to the charging station's output. (c) If the charging station has PPS capability, it can act as a constant current LED driver.

6. Task Light

6.1. Modifications for DC Input

Task lights in a workspace can benefit from localized low-voltage DC distribution. Many USB task lights in today's market are powered by a 5 V USB-A port and use a ballast resistor for current control, as shown in Fig. 13a. The ballast resistor makes the lamp inefficient, susceptible to input voltage swing, and difficult to dim. Advanced task lights overcome these difficulties with an LED driver. Future lamps may be powered by a USB-C charging station, as shown in Fig. 13b.

A further improvement is possible, shown in Fig. 13c, in which the charging station becomes the LED driver. This solution requires a charging station that supports USB protocols with a programmable power supply (PPS) capability (USB-PD 3.0 or QC 3.0). These lamps need only to sense the LED current and program the supply voltage accordingly. This method effectively removes the LED driver conversion stage, while still offering all its benefits.

Figure 14: Prototype of the driverless USB task light.

6.2. Experimental Prototype and Results

The task light prototype, shown in Fig. 14, demonstrates the driverless topology in Fig. 13c. It connects to an Anker PowerPort charger with QC 3.0 (USB-PD 3.0 was not available during this experiment). The Anker PowerPort provides up to 12 V to three 1.5 A LEDs (Cree MTG7-001I-XTE00-NW-0GE3). At the brightest operating point, the LEDs draw 1.5 A at 14.3 W (9.815 V). An Arduino microcontroller generates the brightness control signals, which are sent via the USB data lines as per the QC protocol [56]. Although this proof-of-concept prototype uses voltage control, current control is generally recommended to account for temperature effects and such.

6.3. Discussion

The prototype effectively uses the charging station as an LED driver, thus reducing the number of power conversions. This method is possible in any point-to-point DC topology that supports a protocol with PPS capability.

7. Zone Lighting

7.1. Modifications for DC Input

Zone lighting systems simultaneously operate many light fixtures, and are often found in office and retail buildings. Traditional LED bulbs have internal drivers, and are designed to plug into

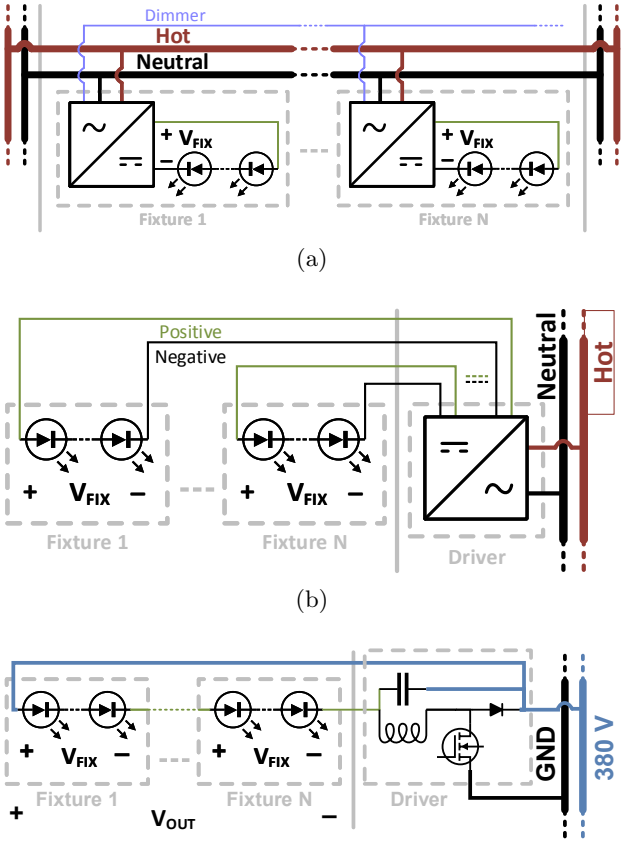

Figure 15: Methods of wiring lighting fixtures. (a) The conventional design with distributed drivers and a dedicated 0-10 V analog dimming line. (b) Most remote driver topologies use an array of parallel current-controlled lines. (c) Series-remote driver topology with a buck-based driver. Although depicted with a DC input, series drivers are currently designed for an AC input. In this topology the number of fixtures N is limited to $N*V_{FIX}<380$ V. Nonetheless, a buck-boost LED driver can allow for more fixtures to be attached.

existing incandescent or fluorescent fixtures. As shown in Fig. 15a, the LED drivers are distributed between the fixtures and may require a separate signaling line for dimming. Although internal LED drivers are standard in AC buildings, they are also present in many of the experimental 380 V DC test beds [26, 27].

External or remote LED drivers are physically separate from the lamp's LEDs, and have applications in outdoors lighting systems such as streetlights and lit signs [57]. Several companies have also started promoting their use in building lighting systems. First, remote drivers reduce component cost since each driver can power several fixtures, as shown in Fig. 15b. Second, easily accessible and replaceable remote drivers reduce maintenance costs, since the driver often limits the lifespan of the entire lamp. Finally, dimming and ancillary functions are more cost-effective with a centralized driver for multiple fixtures.

Figure 16: Prototype of the series-remote driver zone light.

Most commercial remote LED drivers use a parallel design, shown in Fig. 15b, which is ideal for applications that require individual fixture control. Another topology, shown in Fig. 15c, uses a single line to power the LED fixtures in series. Series drivers are uncommon, and the few companies that develop them seldom intend them for an application in indoor zone lighting.

This work aims to demonstrate that series-remote drivers are an excellent design for zone lighting in 380 V DC buildings due to their low overall cost and high efficiency. The cost benefit is a result of using simple low-power hardware to drive many fixtures, as shown in Fig. 15c. In addition, the driver's total switch stress does not increase with the number of fixtures, implying a constant hardware cost.

Series-remote drivers can also be significantly more efficient than their parallel counterparts. In general, buck converters are most efficient at a high MOSFET conduction duty cycle, which happens when the output voltage is closely matched to the input. The drivers in Figs. 15a and 15b undergo a significant step-down from the mains to the fixture voltage V_{FIX}. In contrast, the series-remote driver in Fig. 15c performs a much lighter step-down when several fixtures are attached.

7.2. Experimental Prototype and Results

A 380 V DC series-remote driver was prototyped using the buck-based topology in Fig. 15c. The prototype, shown in Fig.16, uses an MP4000 controller, a 600 V IGBT, and a 10 mH inductor. The experimental fixtures are a set of 75 V 18 W four-foot T8 LED tubes, which come from removing the driver of a PT-T84FP18W. As shown in Fig. 17, the driver's efficiency increases with the number of tubes. For reference, the original tube-integrated AC LED driver, shown in Fig. 18, operates at 92% efficiency and 0.97 power factor.

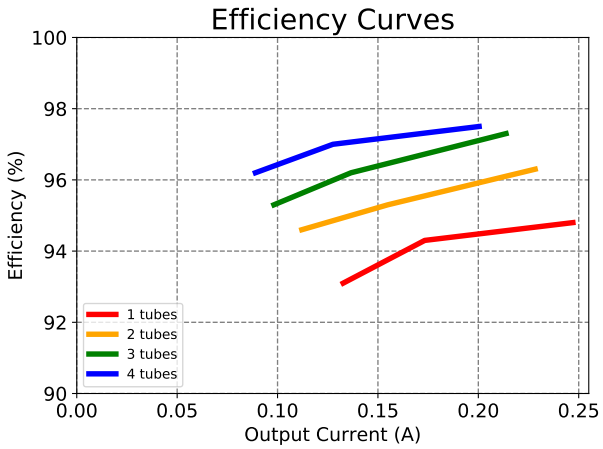

Figure 17: Efficiency curves for the 380 V DC series-remote driver with 1-4 LED tubes attached in series. The driver's efficiency increases with the number of attached tubes.

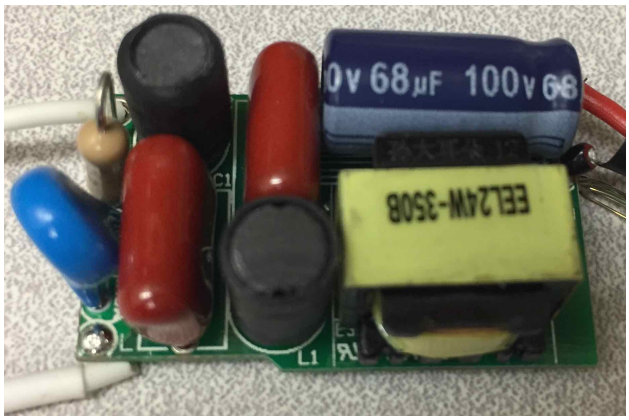

Figure 18: Original AC LED driver packaged in a PT-T84FP18W four-foot LED tube. The board dimensions are 3.5 x 2 cm.

7.3. Discussion

Remote drivers have many advantages over conventional internal drivers, such as cost, maintenance, and control functionality. However, the main drawback is a loss of the plug-and-play simplicity of traditional light bulbs. In addition, remote systems may experience voltage drop over long wire runs. Series-remote drivers add the potential to further improve on hardware costs and efficiency. Nonetheless, their drawbacks include non-trivial wiring and the inability to dim individual fixtures. As such, series-remote drivers are best suited for commercial zone lighting. Overall, further study is required to fully determine the value of series-remote drivers in industry applications.

One potential concern with series fixtures is that a single LED failure would disable the entire multi-fixture string. This drawback can be overcome by equipping each fixture with a bypass

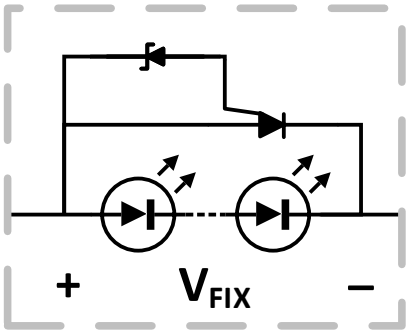

Figure 19: Bypass circuit for the LED fixtures connected to a series-remote driver. This circuit will allow other fixtures to remain powered despite a failure in the series string.

circuit. An example bypass circuit, shown in Fig. 19, is based on a design for bypassing individual LEDs [58]. In this case, the SCR and Zener diode would be sized such that their breakdown voltage is greater than the nominal LED fixture voltage.

Although the prototype only allows five 18 W 75 V tubes to be stacked in series, newer high-brightness LEDs provide more power with less voltage drop [59, 60]. For example, an 18 W bulb with three modern 6 V 1 A LEDs would only drop 18 V. Twenty-one such bulbs would stack to 380 V, which is enough to cover a moderately sized room. A buck-boost series-remote driver allows the flexibility of even more bulbs at the incremental cost of efficiency and safety.

8. Conclusion

Buildings with DC power have taken the recent spotlight in research, but the development of highly efficient DC-ready loads has lagged. This work categorizes the types of loads whose efficiency directly benefits from a DC input. Several types of loads are studied, and some of them are modified or prototyped as direct-DC. This work focuses on low-power residential and small commercial loads, which include a bath fan, refrigerator, wall adapter, task lamp, and zone lighting system. The main focus of each design is to leverage DC input to eliminate or improve the conversion stages.

This project obtained new insights specific to the categories of motor loads, electronics, and lighting. In motor loads, the most efficient type of BLDC motor is designed such that its internal DC capacitor bus is coupled to the DC input. Although there is very little loss across a diode bridge rectifier, a PFC boost rectifier is notably less efficient. In electronics, DC distribution can allow

for downsizing or eliminating wall adapters. The efficiency benefits generally favor DC, though the comparisons must be made with careful attention to the distribution voltage and conversion process. In lighting, DC task lamps can leverage a USB-PD charging station as an LED driver. Zone lighting can benefit greatly from series-remote drivers, but further research must validate their feasibility. In all loads, DC input will improve power quality and reduce the size of the DC capacitors. Further study is required to determine the full value of these secondary effects.

Appendix A. DC Voltage Standards

USB-C is emerging as the single standard and connector for consumer electronics. Its point-to-point power delivery architecture allows for simultaneous power and communications. Power over USB-C strictly adheres to the USB power delivery (USB-PD) protocol [61]. Past USB-PD standards set the programmable voltage to 5 V, 9 V, 15 V, or 20 V. However, as of USB-PD 3.0 (2018), the port can now function as a programmable power supply (PPS) and outputs voltages between 3 V and 21 V with 20 mV increments. USB-C connectors contain twenty-four pins of which eight are for power, two are for dedicated USB-PD communications, and the rest are for data. Due to voltage drop and wire loss inherent with low-voltage distribution, USB is best suited for short-range power distribution such as a cubicle.

Another competing USB protocol is Qualcomm Quick Charge (QC) [62]. QC works with traditional USB-A or B ports, but requires the data lines for power control signaling. It also has a PPS capability with 200 mV increments (QC 3.0), allowing it to charge batteries quickly and efficiently. Although fast charging made QC popular, USB-PD 3.0 now has much of the same functionality. Recent versions of QC also support USB-PD, and these standards may eventually merge.

Although Power over Ethernet (PoE) nominally operates at 48 V, it allows up to 56 V to compensate for wire drop [63–65]. The 802.3bt Type 4 standard allows PoE to transfer 100 W of power over Category 5 Ethernet cable using 4-pair power transfer mode. PoE can be found in phones, cameras, routers, LED luminaires, and other electronics that require power and communications. Since many buildings are already wired with Ethernet cables, PoE represents one of the easiest ways for DC power distribution to enter the market. In addition, PoE operates near the OSHA touch-safe limit (50 V), thus optimally minimizing wire loss while ensuring safety. While USB is best suited to power a work space, PoE can extend to multiple rooms or even an entire residence.

The European Standardization Institute (ETSI) and the EMerge Alliance have established DC standards with specifications for powering datacenters at 380 V DC [66–69]. This standard allows for easy retrofitting since 380 V DC has similar insulation requirements with 277 V AC. Besides datacenters, 380 V DC holds much promise for powering other high-power loads, and allows for efficient coupling with solar and storage [21].

Appendix B. DC Capacitor Voltage in BLDC Motors

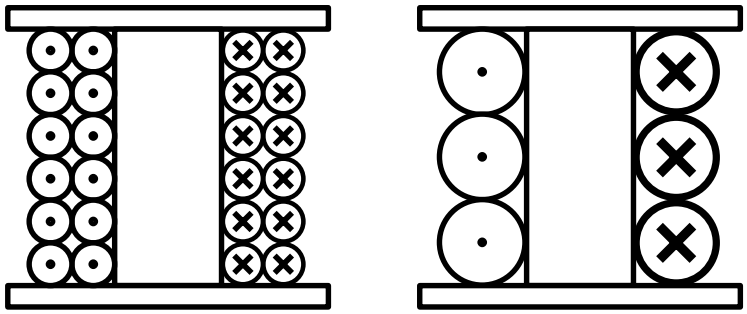

(a) (b)

Figure B.20: Winding area diagram for two motors with equal input power and magnetic flux. The winding area in both motors is roughly equal. In this example, $K = 4$. (a) A high-voltage motor that requires 12 windings, but they can be relatively thin. (b) An equivalent low-voltage motor only requires 3 windings, but they must be thick enough for the relatively high winding current.

Brushless DC (BLDC) motors are designed with a specific AC voltage across the stator windings. The winding voltage dictates the inverter's DC capacitor bus voltage, which can be DC-connected if it equals the DC distribution voltage. This section shows how a motor's winding voltage can be designed independently of its power rating, and can ultimately be designed as a DC-connected device.

For a given application, assume the motor's electrical input power P_{const} is specified and constant. Also assume the motor's magnetic flux ϕ_{const} is constant and is directly related to the mechanical output power. The relations between the electrical stator windings and the magnetic core are:

$$P_{const} = VI \tag{B.1}$$

$$\phi_{const} = \frac{NI}{\mathcal{R}_{tot}} \tag{B.2}$$

$$E = N\frac{d\phi_{const}}{dt}, \tag{B.3}$$

where V and I respectively are the winding's input voltage and current, N is the number of windings, $\mathcal{R}_{tot}$ is the total reluctance of the magnetic core, and E is the back EMF generated in the windings.

Consider a comparison between motors 1 and 2, which both have the same input power $P_1 = P_2$, and magnetic flux $\phi_1 = \phi_2$. However, the main difference is that the winding voltage of motor 1 is designed to be K times greater than that of motor 2. Since $V_1 = KV_2$, Eq. B.1 assures that $I_1 = \frac{1}{K} I_2$. If the two motors are specified with the same magnetic flux and core parameters, then Eq. B.2 requires that $N_1 = KN_2$. In other words, the motor 1 requires K times as many windings, but the windings only pass $\frac{1}{K}$ times as much current. Finally, Eq. B.3 follows that $E_1 = KE_2$, but since $V_1 = KV_2$, then each motor has proportionally as much voltage headroom, and each motor can attain the same maximum speed.

Overall, high-voltage motors use less current and have more stator windings than low-voltage motors of the same input power and flux. The low-voltage motor requires thick high-current windings, but the overall winding packing window is still comparable between the two motors, as shown in Fig. B.20.

Finally, the losses in the high and low-voltage motors are also equivalent. The core loss is equivalent because the flux ϕ is the same between the motors. For winding loss, the factor K falls out of the equations:

$$P_w = I^2 R_w \tag{B.4}$$

$$R_w = \rho \frac{L}{A}. \tag{B.5}$$

The wire loss power P_w and resistance R_w are dependent on the wire length L, cross sectional area A, and resistivity ρ. As shown in Fig. B.20, the number of turns $N_1 = KN_2$ requires motor 1 to have a smaller area $A_1 = \frac{1}{K} A_2$, and greater length $L_1 = KL_2$. As such, motor 1 has a greater wire resistance $R_1 = K^2 R_2$. Nonetheless, the winding current $I_1 = \frac{1}{K} I_2$, and so the overall winding loss power $P_1 = I_1^2 R_1 = (\frac{1}{K} I_2)^2 (K^2 R_2) = P_2$.

Appendix C. Sizing the DC Capacitor Bus

Most types of native-DC loads contain an internal DC capacitor bus, whose size can often be reduced in converting to a direct-DC input. These capacitors are sized such that the peak-to-peak

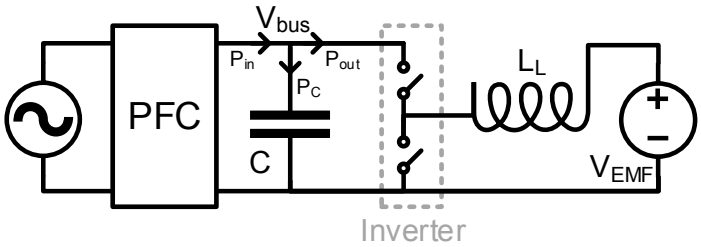

Figure C.21: A model of the energy flow in a VFD motor with PFC. The DC capacitor is responsible for absorbing the AC component of P_{in}, allowing for a purely DC P_{out}. In this model, the inverter is a half-bridge and the motor is represented by its winding inductance L_L and a constant back EMF.

bus voltage ripple, ΔV_C, is within specification. In native-DC loads, the DC capacitor bus is required for:

- Filtering the 120 Hz power ripple from the AC input
- Filtering the inverter PWM current
- Providing an energy buffer for a change in load

In direct-DC loads, the DC capacitor bus is only responsible for the latter two. This section explains how to analytically determine the requisite capacitance for VFD motor loads. It follows with a design example that shows how direct-DC can reduce the bus capacitors.

Appendix C.1. 120 Hz Power Ripple from the AC Input

Many devices require power factor correction (PFC), including electronics over 75 W and all types of lighting. PFC rectifiers control the input current to be sinusoidal and in-phase with the 60 Hz input voltage. As such, the input power is a raised sinusoid at 120 Hz. As shown in Figure C.21, the DC capacitor bus is responsible for absorbing the AC component of the input power P_{in}. To allow for a DC output power P_{out}, the power into the capacitor P_C must be:

$$P_{C,AC} = P_{in,AC+DC} - P_{out,DC} = -P_{in}cos(2\omega_0 t) \tag{C.1}$$

From P_C, the capacitor bus voltage ripple ΔV_C can be solved by an energy analysis [70]:

$$\Delta V_C = \frac{P_{in,avg}}{V_{DC}\omega_0 C}, \tag{C.2}$$

where V_{DC} is the DC bus voltage.

Appendix C.2. Bus voltage ripple from the Inverter

In this analysis, the inverter is a half-bridge circuit with PWM switching frequency f. As shown in Fig. C.21, the half-bridge switches the output between the positive and negative terminals of the DC bus. This switching leads to a swing in output current ΔI_L, which the DC capacitor must ultimately absorb. Salcone and Bond [71] derive the bus voltage ripple as a function of the DC capacitor:

$$\Delta I_L = i_C = \frac{D(1-D)V_{DC}}{fL_L} \tag{C.3}$$

$$\Delta V_C = \frac{V_{DC}}{32L_L C f^2}, \tag{C.4}$$

where L_L is the load or winding inductance, and a duty cycle of $D = 0.5$ results in the largest ripple current.

Appendix C.3. Energy buffer for a change in load

In some applications, the DC capacitor is responsible for maintaining the bus voltage over loading transients. For example, transients in VFD motors may arrise from braking, sudden changes in torque, and start-up. This work develops a simple model to determine the effect of load transients on the bus voltage. As shown in Fig. C.22, the model accounts for the line inductance L_S, which is assumed to be 19.41 μH for 20 m of 10 AWG copper wire. The load transient $I_L(t)$ can be a step $Mu(t)$ or a ramp $Ntu(t)$. The system in Fig. C.22 is represented by the differential equation:

$$L_S C \frac{d^2 v_C}{dt^2} + v_C = V_S - L_S \frac{dI_L(t)}{dt} \tag{C.5}$$

Although realistic systems have a damping component, this model is sufficient to find the worst-case ripple on v_C. The solutions to Eq. C.5 are:

$$I_L(t) = Mu(t) \Rightarrow v_C = V_S - M\sqrt{\frac{L_S}{C}} sin(\frac{t}{\sqrt{L_S C}})$$

$$\Delta V_C = 2M\sqrt{\frac{L_S}{C}} \tag{C.6}$$

$$I_L(t) = Ntu(t) \Rightarrow v_C = V_S - NL_S + NL_S cos(\frac{t}{\sqrt{L_S C}})$$

$$\Delta V_C = 2NL_S. \tag{C.7}$$

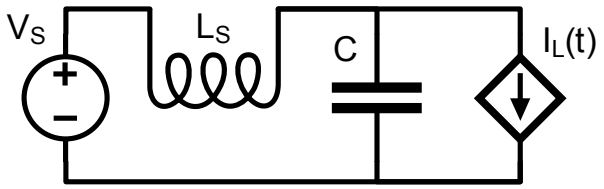

Figure C.22: Simple model of a DC load connected to DC distribution with line inductance L_S and supply voltage V_S. This model examines the input capacitor voltage ripple subject to a current step or ramp.

Table C.3: DC bus voltage ripple due to each effect

C (uF)	AC Ripple (V)	PWM Ripple (V)	Transient Ripple (V)
10.0	78.02	3.32	0.82
100.0	7.8	0.33	0.26
1000.0	0.78	0.03	0.08

As shown in Eq. C.7, the voltage ripple ΔV_C of the ramp response is actually independant of C. As such, Appendix C.4 only accounts for the step response.

The step response magnitude varies with application and technology. Many of the loads in Fig. 2 have nearly constant power draw, and transients only arise at start-up. VFD inverters can soft-start the motor with a low-voltage AC output, allowing for a start-up current that is always lower than the full-load current ($M = I_{out,max}$) [72].

Appendix C.4. Comparison and Discussion

This section uses the LG inverter refrigerator as a design example for comparing the three metrics for capacitor sizing. As discussed in Section 4, the refrigerator draws as much as $P_{in} = 80$ W from a standard 60 Hz AC distribution. The inverter operates at $f = 20$ kHz, and is powered from a DC bus at $V_{DC} = 340$ V. Finally, the compressor's load inductance is dominated by a load-side reactor with $L_L = 0.8$ mH.

As shown in Table C.3, the DC bus voltage ripple ΔV caused by the AC input is considerably greater than the other two sources. With direct-DC input, the DC capacitors can be reduced a factor of ten to twenty. Applications with high input power P_{in} or low bus voltage V_{DC} are especially favorable for direct-DC.

Acknowledgements

This work was supported by the California Energy Commissions EPIC Project EPC-15-024. The authors would like to thank Alan Meier, Leo Rainer, Bruce Nordman, Wei Feng, Chris Marnay, Vagelis Vossos, and Seth Sanders for their technical advice and support. Special thanks to the reviewers and editors.

References

[1] K. Garbesi, V. Vossos, and H. Shen, "Catalog of DC Appliances and Power Systems," Tech. Rep. LBNL-5364E, Lawrence Berkeley National Laboratory, Berkeley, CA, 2011.

[2] A. Perea, C. Honeyman, S. Kann, A. Mond, M. Shiao, S. Rumery, and A. Holm, "U.S. Solar Market Insight: 2016 Year in Review - Executive Summary," tech. rep., GTM Research & Solar Energy Industries Association, Mar. 2017.

[3] G. Research, "U.S. Energy Storage Monitor: Q4 2016 Executive Summary," tech. rep., GTM Research, Dec. 2016.

[4] K. George, "DC Power Production, Delivery and Utilization: An EPRI White Paper," 2006.

[5] G. AlLee and W. Tschudi, "Edison Redux: 380 Vdc Brings Reliability and Efficiency to Sustainable Data Centers," *IEEE Power and Energy Magazine*, vol. 10, pp. 50–59, Nov. 2012.

[6] S. Backhaus, G. W. Swift, S. Chatzivasileiadis, W. Tschudi, S. Glover, M. Starke, J. Wang, M. Yue, and D. Hammerstrom, "DC Microgrids Scoping Study Estimate of Technical and Economic Benefits," Tech. Rep. LAUR1522097, Los Alamos National Laboratory, Mar. 2015.

[7] P. Savage, R. R. Nordhaus, and S. P. Jamieson, "From Silos to Systems: Issues in Clean Energy and Climate Change: DC microgrids: benefits and barriers," tech. rep., Yale School of Forestry & Environmental Sciences, 2010.

[8] D. Denkenberger, D. Driscoll, E. Lighthiser, P. May-Ostendorp, B. Trimboli, and P. Walters, "DC Distribution Market, Benefits, and Opportunities in Residential and Commercial Buildings," tech. rep., Pacific Gas & Electric Company, Oct. 2012.

[9] A. Sannino, G. Postiglione, and M. Bollen, "Feasibility of a DC network for commercial facilities," *IEEE Transactions on Industry Applications*, vol. 39, pp. 1499–1507, Sept. 2003.

[10] B. A. Thomas, I. L. Azevedo, and G. Morgan, "Edison Revisited: Should we use DC circuits for lighting in commercial buildings?," *Energy Policy*, vol. 45, pp. 399–411, June 2012.

[11] V. Vossos, K. Garbesi, and H. Shen, "Energy savings from direct-DC in U.S. residential buildings," *Energy and Buildings*, vol. 68, Part A, pp. 223–231, Jan. 2014.

[12] K. Engelen, E. Leung Shun, P. Vermeyen, I. Pardon, R. D'hulst, J. Driesen, and R. Belmans, "The Feasibility of Small-Scale Residential DC Distribution Systems," in *IECON 2006 - 32nd Annual Conference on IEEE Industrial Electronics*, pp. 2618–2623, Nov. 2006.

[13] B. Glasgo, I. L. Azevedo, and C. Hendrickson, "How much electricity can we save by using direct current circuits in homes? Understanding the potential for electricity savings and assessing feasibility of a transition towards DC powered buildings," *Applied Energy*, vol. 180, pp. 66–75, Oct. 2016.

[14] D. Hammerstrom, "AC Versus DC Distribution Systems. Did We Get it Right?," in *IEEE Power Engineering Society General Meeting, 2007*, pp. 1–5, June 2007.

[15] Z. Liu and M. Li, "Research on Energy Efficiency of DC Distribution System," *AASRI Procedia*, vol. 7, pp. 68–74, 2014.

[16] M. Noritake, H. Hoshi, K. Hirose, H. Kita, R. Hara, and M. Yagami, "Operation algorithm of DC microgrid for achieving local production for local consumption of renewable energy," in *Telecommunications Energy Conference 'Smart Power and Efficiency' (INEC), Proceedings of 2013 35th International*, pp. 1–6, Oct. 2013.

[17] M. Noritake, K. Yuasa, T. Takeda, H. Hoshi, and K. Hirose, "Demonstrative research on DC microgrids for office buildings," in *Telecommunications Energy Conference (INEC), 2014 IEEE 36th International*, pp. 1–5, Sept. 2014.

[18] P. Paajanen, T. Kaipia, and J. Partanen, "DC supply of low-voltage electricity appliances in residential buildings," in *CIRED 2009 - 20th International Conference and Exhibition on Electricity Distribution - Part 1*, pp. 1–4, June 2009.

[19] M. Starke, L. Tolbert, and B. Ozpineci, "AC vs. DC distribution: A loss comparison," in *Transmission and Distribution Conference and Exposition, 2008. T #x00026;D. IEEE/PES*, pp. 1–7, Apr. 2008.
[20] S. Willems and W. Aerts, *Study and Simulation Of A DC Micro Grid With Focus on Efficiency, Use of Materials and Economic Constraints*. PhD thesis, University of Leuven, Leuven, Belgium, 2014.
[21] D. L. Gerber, V. Vossos, W. Feng, C. Marnay, B. Nordman, and R. Brown, "A simulation-based efficiency comparison of ac and dc power distribution networks in commercial buildings," *Applied Energy*, vol. 210, pp. 1167 – 1187, 2018.
[22] D. L. Gerber, V. Vossos, W. Feng, A. Khandekar, C. Marnay, and B. Nordman, "A simulation based comparison of ac and dc power distribution networks in buildings," in *2017 IEEE Second International Conference on DC Microgrids (ICDCM)*, pp. 588–595, June 2017.
[23] V. Vossos, D. Gerber, Y. Bennani, R. Brown, and C. Marnay, "Techno-economic analysis of dc power distribution in commercial buildings," *Applied Energy*, vol. 230, pp. 663 – 678, 2018.
[24] S. M. Frank and S. Rebennack, "Optimal design of mixed ac-dc distribution systems for commercial buildings: A nonconvex generalized benders decomposition approach," *European Journal of Operational Research*, vol. 242, no. 3, pp. 710 – 729, 2015.
[25] R. Weiss, L. Ott, and U. Boeke, "Energy efficient low-voltage DC-grids for commercial buildings," in *2015 IEEE First International Conference on DC Microgrids (ICDCM)*, pp. 154–158, June 2015.
[26] U. Boeke and M. Wendt, "DC power grids for buildings," in *2015 IEEE First International Conference on DC Microgrids (ICDCM)*, pp. 210–214, June 2015.
[27] D. Fregosi, S. Ravula, D. Brhlik, J. Saussele, S. Frank, E. Bonnema, J. Scheib, and E. Wilson, "A comparative study of DC and AC microgrids in commercial buildings across different climates and operating profiles," in *2015 IEEE First International Conference on DC Microgrids (ICDCM)*, pp. 159–164, June 2015.
[28] N. P. Systems, "Fort Belvoir Direct Coupling DC Microgrid."
[29] M. Wright, "Eaton demonstrates distributed DC power for LED lighting at LFI," *LEDs Magazine*, May 2016.
[30] H. Kakigano, Y. Miura, and T. Ise, "Low-voltage bipolar-type dc microgrid for super high quality distribution," *IEEE Transactions on Power Electronics*, vol. 25, pp. 3066–3075, Dec 2010.
[31] Y. Ito, Y. Zhongqing, and H. Akagi, "Dc microgrid based distribution power generation system," in *The 4th International Power Electronics and Motion Control Conference, 2004. IPEMC 2004.*, vol. 3, pp. 1740–1745 Vol.3, Aug 2004.
[32] V. Vossos, S. Pantano, R. Heard, and R. Brown, "Dc appliances and dc power distribution," 2017.
[33] A. Mishra, K. Rajeev, and V. Garg, "Assessment of 48 volts dc for homes," in *2018 IEEMA Engineer Infinite Conference (eTechNxT)*, pp. 1–6, IEEE, 2018.
[34] M.-H. Ryu, H.-S. Kim, J.-W. Baek, H.-G. Kim, and J.-H. Jung, "Effective test bed of 380-v dc distribution system using isolated power converters," *IEEE transactions on industrial electronics*, vol. 62, no. 7, pp. 4525–4536, 2015.
[35] G. Makarabbi, V. Gavade, R. Panguloori, and P. Mishra, "Compatibility and performance study of home appliances in a dc home distribution system," in *Power Electronics, Drives and Energy Systems (PEDES), 2014 IEEE International Conference on*, pp. 1–6, IEEE, 2014.
[36] M. Noritake, K. Yuasa, T. Takeda, K. Shimomachi, R. Hara, H. Kita, and T. Matsumura, "Experimental study of a 400 v class dc microgrid for commercial buildings," in *Power Electronics and ECCE Asia (ICPE-ECCE Asia), 2015 9th International Conference on*, pp. 1730–1735, IEEE, 2015.
[37] A. Stippich, A. Sewergin, G. Engelmann, J. Gottschlich, M. Neubert, C. van der Broeck, P. Schuelting, R. Goldbeck, and R. De Doncker, "From ac to dc: Benefits in household appliances," in *International ETG Congress 2017; Proceedings of*, pp. 1–6, VDE, 2017.
[38] A. Jhunjhunwala, K. Vasudevan, P. Kaur, B. Ramamurthi, S. Bitra, K. Uppal, *et al.*, "Energy efficiency in lighting: Ac vs dc led lights," in *Sustainable Green Buildings and Communities (SGBC), International Conference on*, pp. 1–4, IEEE, 2016.
[39] M. G. Jahromi, G. Mirzaeva, S. D. Mitchell, and D. Gay, "Dc power vs ac power for mobile mining equipment," in *Industry Applications Society Annual Meeting, 2014 IEEE*, pp. 1–8, IEEE, 2014.
[40] D. Das, N. Kumaresan, V. Nayanar, K. N. Sam, and N. A. Gounden, "Development of bldc motor-based elevator system suitable for dc microgrid," *IEEE/ASME Transactions on Mechatronics*, vol. 21, no. 3, pp. 1552–1560, 2016.
[41] R. K. Chauhan, C. Phurailatpam, B. Rajpurohit, F. Gonzalez-Longatt, and S. Singh, "Demand-side management system for autonomous dc microgrid for building," *Technology and Economics of Smart Grids and Sustainable Energy*, vol. 2, no. 1, p. 4, 2017.
[42] K. Yukita, T. Hosoe, S. Horie, T. Matsumura, M. Hamanaka, K. Hirose, and M. Noritake, "Air conditioning

equipment using dc power supply system," in *Telecommunications Energy Conference (INTELEC), 2017 IEEE International*, pp. 229–232, IEEE, 2017.

[43] P. Rani, D. Vignesh, S. Gunaki, and A. Jhunjhunwala, "Design of converters for leveraging 48v dc power line at homes/offices," in *Sustainable Green Buildings and Communities (SGBC), International Conference on*, pp. 1–5, IEEE, 2016.

[44] O. Lucia, I. Cvetkovic, H. Sarnago, D. Boroyevich, P. Mattavelli, and F. C. Lee, "Design of home appliances for a dc-based nanogrid system: An induction range study case," *IEEE Journal of Emerging and Selected Topics in Power Electronics*, vol. 1, no. 4, pp. 315–326, 2013.

[45] OSHA 1910.303(g)(2)(i), "Guarding requirements for 50 volts or more DC," standard, Occupational Safety and Health Administration, Washington, D.C., 2015.

[46] BS 7671:2008, "Requirements for Electrical Installations. IET Wiring Regulations," standard, Institution of Engineering and Technology, Stevenage, England, 2015.

[47] R. Saidur, S. Mekhilef, M. B. Ali, A. Safari, and H. Mohammed, "Applications of variable speed drive (vsd) in electrical motors energy savings," *Renewable and Sustainable Energy Reviews*, vol. 16, no. 1, pp. 543–550, 2012.

[48] J. A. Rooks and A. K. Wallace, "Energy efficiency of vsds," *IEEE Industry Applications Magazine*, vol. 10, no. 3, pp. 57–61, 2004.

[49] M. Didden, J.-M. De Hoe, J. Callebaut, and E. De Jaeger, "Installing variable speed drives: Energy efficiency profits versus power quality losses," in *Electricity Distribution, 2005. CIRED 2005. 18th International Conference and Exhibition on*, pp. 1–5, IET, 2005.

[50] H. C. Emissions, "Guidelines to the standard en 61000-3-2," *European Power Supply Manufacturers Association*, 2010.

[51] I. IEC, "61000-3-2: 2014 electromagnetic compatibility (emc)-part3-2: Limits-limits for harmonic current emissions (equipment input current 16a per phase)," *British Standards Institute*, 2014.

[52] L. Gu, X. Ruan, M. Xu, and K. Yao, "Means of eliminating electrolytic capacitor in ac/dc power supplies for led lightings," *IEEE Transactions on Power Electronics*, vol. 24, no. 5, pp. 1399–1408, 2009.

[53] W. Chen and S. R. Hui, "Elimination of an electrolytic capacitor in ac/dc light-emitting diode (led) driver with high input power factor and constant output current," *IEEE Transactions on Power Electronics*, vol. 27, no. 3, pp. 1598–1607, 2012.

[54] CUI Inc, "Efficiency standards for external power supplies."

[55] SL Power Electronics, "Energy efficiency requirements by levels." Application Note: AN-G-001/15.

[56] V. Deconinck, "Turning a quick charge 3.0 charger into a variable voltage power supply."

[57] 1000bulbs.com, "Understanding led drivers," May 2014.

[58] K. Bollmann and T. C. Penick, "Led lighting system with bypass circuit for failed led," Apr. 2 2013. US Patent 8,410,705.

[59] S. Keeping, "High current, high brightness leds simplify power supply solutions," February 2012.

[60] D. Solly, "Driving high intensity led strings in dc to dc applications," 2007.

[61] "Universal Serial Bus Power Delivery Specification, Version 1.2, Revision 3.0," standard, June 2018.

[62] Qualcomm, "Quick Charge 3.0 specs," standard.

[63] F. G. Osorio, M. Xinran, Y. Liu, P. Lusina, and E. Cretu, "Sensor network using power-over-ethernet," in *Computing and Communication (IEMCON), 2015 International Conference and Workshop on*, pp. 1–7, IEEE, 2015.

[64] J. Petroski, "Power over ethernet thermal analysis with an engineering mechanics approach," in *Thermal Measurement, Modeling & Management Symposium (SEMI-THERM), 2016 32nd*, pp. 50–56, IEEE, 2016.

[65] J. Johnston, J. Counsell, G. Banks, and M. J. Stewart, "Beyond power over ethernet: The development of digital energy networks for buildings," in *CIBSE Technical Symposium 2012-Buildings Systems and Services for the 21st Century*, pp. Session–5, 2012.

[66] E. Alliance, "380 Vdc Architectures for the Modern Data Center," *EMerge Alliance, San Ramon, CA, USA*, 2013.

[67] D. E. Geary, D. P. Mohr, D. Owen, M. Salato, and B. Sonnenberg, "380V DC eco-system development: present status and future challenges," in *Telecommunications Energy Conference'Smart Power and Efficiency'(INTELEC), Proceedings of 2013 35th International*, pp. 1–6, VDE, 2013.

[68] D. J. Becker and B. Sonnenberg, "DC microgrids in buildings and data centers," in *Telecommunications Energy Conference (INTELEC), 2011 IEEE 33rd International*, pp. 1–7, IEEE, 2011.

[69] EN ETSI, "Environmental Engineering (EE); Power supply interface at the input to telecommunications and datacom (ICT) equipment; Part 3: Operated by rectified current source, alternating current source or direct current source up to 400 V; Sub-part 1: Direct current source up to 400 V," *European standard EN 300 132-3-1*

V2.1.1, pp. 2012–02.

[70] D. L. Gerber, C. Le, M. Kline, S. Sanders, and P. Kinget, "An integrated multilevel converter with sigma-delta control for led lighting," *IEEE Transactions on Power Electronics*, pp. 1–1, 2018.

[71] M. Salcone and J. Bond, "Selecting film bus link capacitors for high performance inverter applications," in *Electric Machines and Drives Conference, 2009. IEMDC'09. IEEE International*, pp. 1692–1699, IEEE, 2009.

[72] W. Lukitsch, "Soft start vs ac drives-understand the differences," in *Textile, Fiber and Film Industry Technical Conference, 1999 IEEE Annual*, pp. 5–pp, IEEE, 1999.